Vol. 18, pp. 317-326 (2021)
doi: 10.2142/biophysico.bppb-v18.038

Biophysics and Physicobiology
https://www.jstage.jst.go.jp/browse/biophysico/

Review Article (Invited)

Unique Cl^- pump rhodopsin with close similarity to H^+ pump rhodopsin

Takashi Kikukawa

Faculty of Advanced Life Science, Hokkaido University, Sapporo, Hokkaido 060–0810, Japan

Received September 24, 2021; Accepted December 20, 2021;
Released online in J-STAGE as advance publication December 22, 2021
Edited by Yoshinori Shichida

Microbial rhodopsin is a ubiquitous membrane protein in unicellular microorganisms. Similar to animal rhodopsin, this protein consists of seven transmembrane helices and the chromophore retinal. However, unlike animal rhodopsin, microbial rhodopsin acts as not only a photosignal receptor but also a light-activated ion transporter and light-switchable enzyme. In this article, the third Cl^- pump microbial rhodopsin will be introduced. The physiological importance of Cl^- pumps has not been clarified. Despite this, their mechanisms, especially that of the first Cl^- pump halorhodopsin (HR), have been studied to characterize them as model proteins for membrane anion transporters. The third Cl^- pump defines a phylogenetic cluster distinct from other microbial rhodopsins. However, this Cl^- pump conserves characteristic residues for not only the Cl^- pump HR but also the H^+ pump bacteriorhodopsin (BR). Reflecting close similarity to BR, the third Cl^- pump begins to pump H^+ outwardly after single amino acid replacement. This mutation activates several residues that have no roles in the original Cl^- pump function but act as important H^+ relay residues in the H^+ pump mutant. Thus, the third Cl^- pump might be the model protein for functional differentiation because this rhodopsin seems to be the Cl^- pump occurring immediately after functional differentiation from the BR-type H^+ pump.

Key words: photobiology, retinal proteins, ion pump, membrane transport

Significance

Microbial rhodopsin is a photoreceptive protein with various functions. These proteins are considered to evolve from H^+ pump-type rhodopsin through extensive optimization of the residues and structures to achieve their respective functions. However, this is not the case for the third Cl^- pump rhodopsin, which seems to be a Cl^- pump that just differentiated from the H^+ pump and has not fully optimized into a mature Cl^- pump. Indeed, this Cl^- pump was converted into a H^+ pump by only single amino acid replacement. The third Cl^- pump might be a model protein to analyze the process of functional differentiation.

Introduction

Most organisms can utilize sunlight as energy and information sources. These capabilities are conferred by photoreceptor proteins, which commonly contain light-absorbing cofactor "chromophores" [1]. Upon illumination, chromophores cause photoisomerization and/or photoreduction, which in turn trigger changes in protein moieties to achieve their respective functions. Rhodopsin is the largest family of photoreceptive proteins that use retinal chromophores (for reviews, see [2-4]). The name "rhodopsin" was originally given to a membrane protein, which acts as a photosensor in the eyes of animals. To date, similar proteins are known to be widespread in all three domains of life, i.e., bacteria, archaea, and eukarya. Based on their amino acid sequences, these rhodopsins can be categorized into two

Corresponding author: Takashi Kikukawa, Faculty of Advanced Life Science, Hokkaido University, N10 W8, Kita-ku, Sapporo, Hokkaido 060–0810, Japan. ORCID iD: https://orcid.org/0000-0002-6185-7281, e-mail: kikukawa@sci.hokudai.ac.jp

groups [5, 6]. One is animal rhodopsin, and the other is microbial rhodopsin. The former mainly functions as photosensors, whereas the other functions as not only photosensors but also light-to-chemical energy converters. Similar to other photoreceptor proteins, rhodopsins can be easily activated by light, and subsequently appearing intermediates can be analyzed by time-resolved techniques and low-temperature trapping methods ([2-4] and references within). Due to these advantages, the mechanisms of various rhodopsins have been extensively studied as model proteins. In particular, for microbial rhodopsins, many members can be easily prepared through recombinant expression in *Escherichia coli* and yeast cells. Moreover, the continuous discovery of new members has further stimulated research interest in microbial rhodopsins [7]. In this article, I introduce a cyanobacterial Cl^- pump rhodopsin, which is the third Cl^- pump [8]. Microbial rhodopsins are considered to evolve from the H^+ pump-type rhodopsin. The cyanobacterial Cl^- pump has a close similarity with the H^+ pump rhodopsin and thus offers insight into protein evolution.

Three Cl^- Pump Rhodopsins

The first microbial rhodopsin identified was an H^+ pump bacteriorhodopsin (BR) from an extremely halophilic haloarchaeon, *Halobacterium salinarum* [9, 10]. Subsequently, a Cl^- pump halorhodopsin (HR) [11, 12] and two photosensing rhodopsins [13, 14] were discovered from the same archaeon. These findings were achieved by performing careful observations of the host organism and its naturally occurring mutants. However, this approach was overtaken by gene analysis methods approximately 20 years ago. Starting in 1999, relatives of archaeal rhodopsins were discovered in various microorganisms through the identification of their genes and were functionally characterized after their heterologous expression [7, 15]. At present, microbial rhodopsins are ubiquitous in unicellular organisms inhabiting various environments and have divergent functions as, for example, light-driven ion pumps, light-gated ion channels, light sensors, and even light-switchable enzymes.

For Cl^- pumps, two groups other than HR have also been identified through gene analyses. However, these identifications were achieved long after the initial discoveries of novel rhodopsins. The second Cl^- pump group was identified in 2014 from the genomes of marine bacteria [16]. This group is designated here as "NTQ rhodopsin" based on the "motif" residue, the details of which will be described below. The host strains belong to large eubacterial categories inhabiting world oceans. Thus, the second Cl^- pump seems to be widely spread in marine environments. The NTQ rhodopsins are phylogenetically close to the Na^+ pump rhodopsin and far from HR and archaeal rhodopsins. Indeed, the overall structure of the NTQ rhodopsin is very close to that of the Na^+ pump rhodopsin [17-20]. Thus, NTQ rhodopsins are considered to have independently evolved from HR. Conversely, the third Cl^- pump, which is designated here as "TSD rhodopsin", is relatively close to archaeal rhodopsins [8].

The Third Cl^- Pump: A Unique Rhodopsin from Terrestrial Cyanobacteria

The third Cl^- pump group was discovered in 2016 from the genomes of cyanobacteria [8]. The host cells are largely confined to inhabitants of terrestrial environments. The first characterized member was a rhodopsin from *Mastigocladopsis repens*, which was named MrHR due to the similarities with HR in terms of anion pump function and motif residues. After recombinant expression in *E. coli* cells, MrHR was revealed to pump only smaller halide ions, Cl^- and Br^-. Conversely, HR and NTQ rhodopsins can also pump I^- and NO_3^- [16, 21-23]. Thus, MrHR has a rather restricted filter for substrate ions. The closed homolog from *Synechocystis* sp. PCC 7509 (SyHR) was secondarily characterized and then revealed to additionally pump SO_4^{2-}, although SyHR cannot pump I^- and NO_3^- [24]. Thus, SO_4^{2-} might be pumped in a different mode compared to that for Cl^- and Br^-. The TSD rhodopsin is relatively close to archaeal rhodopsins phylogenetically and conserves not only the residues essential for HR but also the residues essential for BR. MrHR is the best characterized member of the TSD rhodopsin, whereas for HR, a member from *Natronomonas pharaonis* (NpHR) was well investigated. Thus, in the following sections, I will describe mainly MrHR in comparison with NpHR and BR.

All microbial rhodopsins have common structural features. They consist of seven transmembrane helices and the retinal, which is bound to a conserved Lys residue on the G helix (the seventh helix) via a protonated Schiff base (PSB; "Schiff base" will be abbreviated as SB). Moreover, all functions are triggered by the same light-induced isomerization of retinal from the all-*trans* to 13-*cis* state. Thus, their respective functions seem to be largely determined by specific residues at appropriate positions. In particular, three specific residues on the C helix are regarded as functionally important and are called "motifs", although the importance of each residue varies depending on the rhodopsin. In the upper panels of Fig. 1, respective motif residues (underlined) are shown in the overall structures of BR, NpHR, MrHR and its T74D mutant (MrHR-T74D), along with other characteristic residues. The PSB regions are expanded in the lower panels, involving the first two motif residues.

For BR, in terms of its "DTD" motif, two Asp residues are especially important (Fig. 1a, e) (for reviews, see [25, 26]). The first "D" residue, corresponding to Asp85, is initially deprotonated in the dark state and thus stabilizes the positively charged PSB as the counterion. Upon illumination, Asp85 acts as an H^+ acceptor from the PSB. This primary H^+ transfer

is essential to evoke multiple subsequent H^+ transfer reactions. The deprotonated SB subsequently captures H^+ from the cytoplasmic (CP) medium. The third "D" residue, corresponding to Asp96 (Fig. 1a), greatly accelerates this H^+ capture process, where the "D" residue first acts as an H^+ donor to SB and then captures another H^+ from the CP medium. When Asp96 is replaced by nondissociable residues, the H^+ capture process is substantially slowed [27]. As a result, the turnover rate of the photocycle is significantly lowered, so the H^+ pump activity under constant illumination becomes negligible. Thus, for BR, the first and third motif residues are essential for the H^+-pumping function.

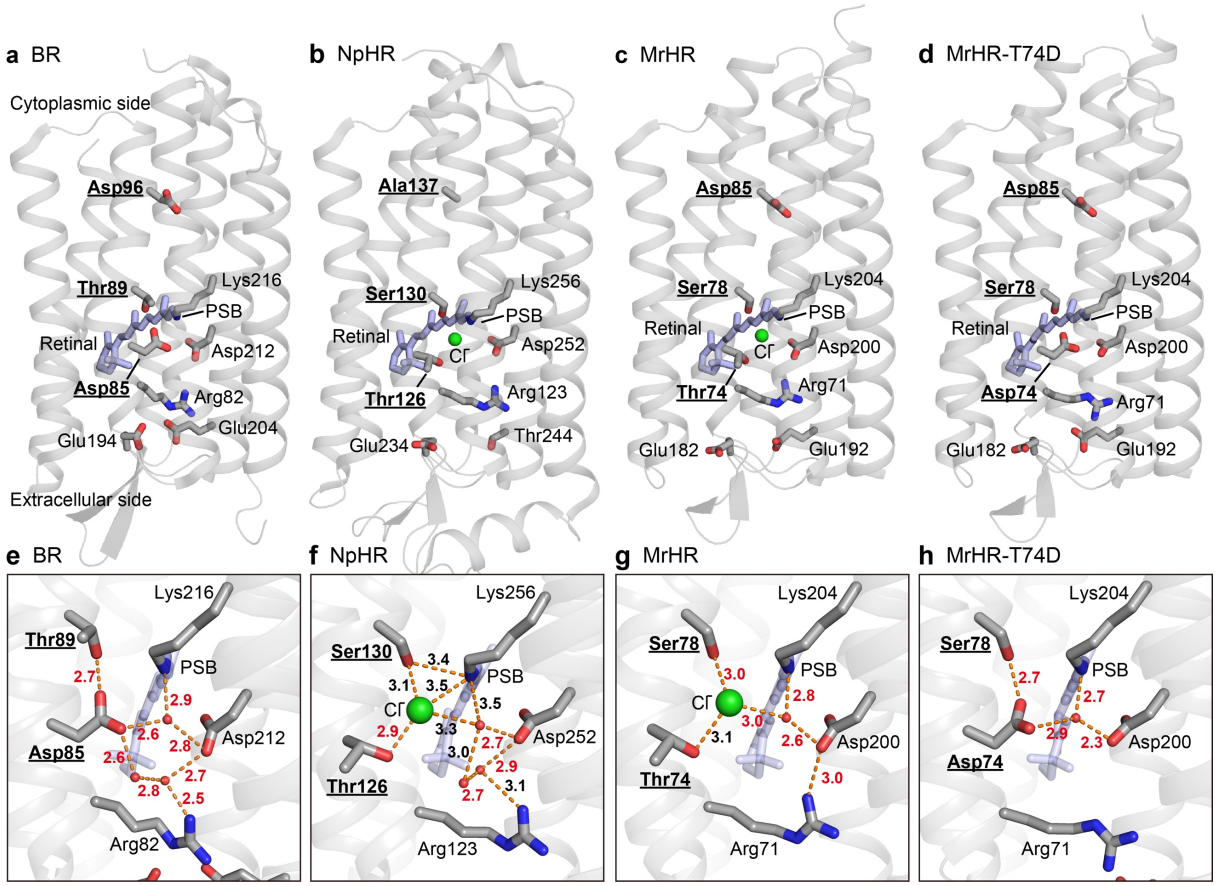

Figure 1 Tertiary structures of BR, NpHR, MrHR and the MrHR-T74D mutant. (a-d) Overall structures are shown with three motif residues, which are underlined, and other characteristic residues. (e-h) The PSB regions are shown with water molecules (red spheres). Broken lines indicate the polar contacts within 3.5 Å among the components shown in the respective panels. Their distances within 3.0 Å are indicated in red, and the longer distances are shown in black. The Protein Data Bank codes are 1C3W for BR, 3A7K for NpHR, 6XL3 for MrHR, and 6WP8 for MrHR-T74D. (a, b, e, f) Adapted by permission from Springer Nature Customer Service Centre GmbH: [28], Copyright Springer Nature Singapore Pte Ltd. (2021).

For the "TSA" motif of NpHR, the first and second residues are important (Fig. 1b, f) [29-31]. In contrast to BR, the first motif residue is "T" in NpHR (i.e., T126). As a result, NpHR can bind Cl^- at this position as the counter ion for the PSB. This Cl^- binding in the dark state is a prerequisite for light-driven Cl^- pump activity. Similar to the first "T", the second "S" residue (S130) directly interacts with Cl^- and contributes to its strong binding in the dark state (Fig. 1f). The "S" residue also appears to be important to guide Cl^- movement during the first half of the photocycle, in which Cl^- gradually moves toward the CP side inside the protein [32]. During this movement, the second "S" also moves its sidechain and maintains the hydrogen bonding interaction with Cl^-. This role cannot be served by other residue. Regardless of the S to T mutation, the photocycle is significantly distorted [29] and loses Cl^- pumping activity (our unpublished result). Thus, the first two motif residues are essential for NpHR. In contrast, the vital role of the third "A" residue, corresponding to Ala137, has not been reported.

MrHR conserves the first two motif residues "TS" in NpHR in the TSD motif (T74 and S78 in MrHR) (Fig. 1c, g). Thus, Cl^--pumping activity was expected for MrHR and then experimentally confirmed as mentioned above [8]. For MrHR,

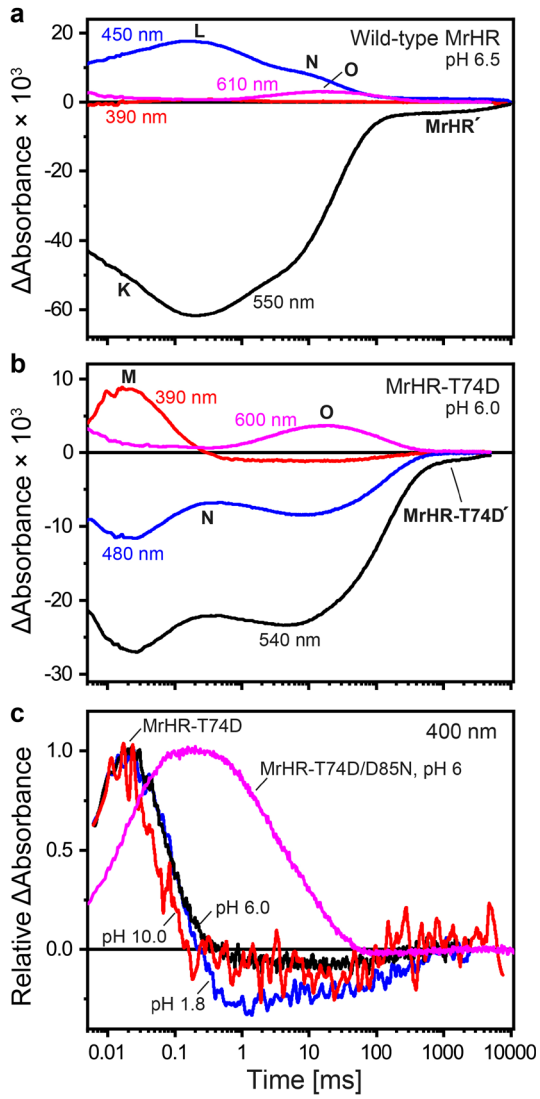

Figure 2 Comparisons of photocycles of wild-type MrHR and the mutants. Flash-induced absorbance changes at selective wavelengths are plotted for (a) wild-type MrHR and (b) the T74D mutant. In Panel (c), time traces at 400 nm, reflecting the M intermediate, are plotted for the T74D and T74D/D85N mutants. No pH dependence of the M decay rate was observed for the T74D mutant until pH 10. For the T74D/D85N mutant, M exhibited significantly slower decay than the T74D mutant, indicating that the D85 residue surely acts as a H^+ donor residue. Adapted by permission from Springer Nature Customer Service Centre GmbH: [28], Copyright Springer Nature Singapore Pte Ltd. (2021).

these "TS" residues were also proven to contribute to strong Cl^- binding in the dark state [33]. The subsequently solved tertiary structure revealed that MrHR has almost the same Cl^--binding site as NpHR (Fig. 1f, g) [34, 35], i.e., in both sites, two motif residues (TS) and Cl^- have almost the same positions and form a hydrogen bonding network with other components, including PSB, water molecules and nearby Asp residues (Asp252 for NpHR; Asp200 for MrHR). Reflecting similar Cl^--binding sites, MrHR and NpHR exhibit similar dissociation constants against halide ions (e.g., for Cl^-, 2 mM for MrHR, 3 mM for NpHR) [8, 36]. Moreover, the photocycles are also similar between MrHR and NpHR [8, 37]. Figure 2a shows the flash-induced absorbance changes of MrHR, which reflect the formation of intermediates and a concomitant decrease in the original dark state. For MrHR, the intermediates have not been deeply characterized compared to those of NpHR. However, judging from the λ_{max} values and the appearance timings, similar intermediates, i.e., K, L, N, and O, seem to appear in both photocycles. Significant exceptions are the last intermediates, MrHR´ and NpHR´. They commonly have absorption spectra similar to those of their respective dark states. However, their decay time constants are significantly different. They are 47 ms for NpHR´ but 5.6 s for MrHR´ [33, 36]. Due to the slow decay of MrHR´, MrHR seems to exhibit weak Cl^--pumping activity under constant illumination. Thus, MrHR appears to be an inefficient Cl^- pump compared to NpHR.

For MrHR, the third motif residue is "D" (D85) (Fig. 1c). Its replacement by Asn and Ala had no effects on Cl^--pumping activity, the photocycle, and the Cl^--binding strength in the dark state [8, 33]. Similarly, no effects were observed for NpHR upon the replacement of the third "A" (TS<u>A</u>) by the Asp residue (our unpublished result). Thus, the third motif residues have no role in either Cl^- pump. However, the "D" for TSD rhodopsin is impressive because it is common to BR (DT<u>D</u>), in which the third D is essential for H^+ pump function. In addition to the third motif residue, MrHR also conserves a characteristic pair, Glu194 and Glu204, in BR (Fig. 1a), which correspond to Glu182 and Glu192 in MrHR (Fig. 1c). In BR, this pair acts as a H^+ releasing group (PRG) to the extracellular (EC) medium and contributes to strong H^+ pump activity [38]. Conversely, the corresponding pair in MrHR has no important role in the Cl^--pumping function, which was confirmed by replacement with Gln residues [33]. Thus, MrHR seems to be the Cl^- pump, which was differentiated from a BR-type H^+ pump, but the residues have not been fully optimized for mature Cl^- pumps.

Functional Conversion of MrHR into an Outward H^+ Pump

In 1995, BR was functionally converted into a Cl^- pump by a single amino acid mutation [39], which was accomplished via the replacement of the first motif residue "D" in BR (<u>D</u>TD) by the corresponding "T" in HR (<u>T</u>SA). However, reverse conversion, i.e., the conversion of HR into a H^+ pump, has not been achieved, even after the introduction of ten mutations [40-42]. Interestingly, this conversion was achieved for MrHR only with the T74D mutation [8], which was the

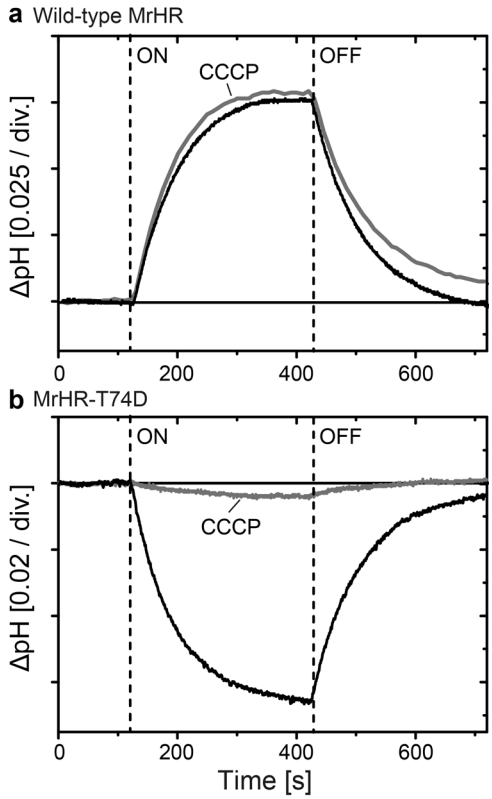

Figure 3 Experimental verification of the functional conversion of MrHR from an inward Cl^- pump to an outward H^+ pump. Light-induced pH changes are plotted for suspensions of *E. coli* cells expressing wild-type MrHR (a) and the T74D mutant (b). (a) Inward Cl^- transport resulted in a pH increase through passive H^+ inflow in response to the interior negative membrane potential. The addition of the protonophore CCCP (10 μM) slightly enhanced the pH increase, reflecting weak Cl^--pumping activity. (b) The MrHR-T74D mutant induced a pH decrease due to outward H^+ pumping activity. The CCCP removed the pH change, indicating that this mutant indeed pumped H^+ outwardly. Data from [8], Copyright 2016 ASBMB. Currently published by Elsevier Inc; originally published by American Society for Biochemistry and Molecular Biology.

replacement of the first motif residue (TSD) by the corresponding "D" in BR (DTD). Thus, this replacement was just a reverse mutation for BR to HR conversion [39] and involved introduction of the H^+ acceptor Asp residue into MrHR. The success of the conversion was clearly proven by the light-induced pH changes of the *E. coli* suspension (Fig. 3) [8]. For the cells expressing wild-type MrHR, illumination induced a pH increase (Fig. 3a), which reflects passive H^+ inflow in response to the interior negative membrane potential created by the inward Cl^--pumping activity. The addition of protonophore carbonyl cyanide m-chlorophenylhydrazone (CCCP) enhanced the pH increase due to the facilitation of H^+ inflow (Fig. 3a), although the enhancement was faint, probably reflecting the small membrane potential created by MrHR. Conversely, for MrHR-T74D, the opposite pH change was observed (Fig. 3b), i.e., illumination induced a pH decrease due to the outward H^+ pumping activity. This pH decrease disappeared with the addition of CCCP, indicating that H^+ was indeed pumped by MrHR-T74D. This mutation was the first successful conversion from the inward Cl^- pump into the outward H^+ pump.

Reflecting the functional conversion, MrHR-T74D exhibited significantly different behaviors from wild-type MrHR. As mentioned above, Cl^- pumps initially bind Cl^- to the vicinity of PSB in the dark state. This Cl^- binding can be easily detected by the spectral shift of retinal absorption. However, for MrHR-T74D, the spectral shift did not occur even in the presence of 500 mM Cl^- [8]. Thus, the embedded Asp residue is deprotonated and acts as the counterion of the PSB. After illumination, this Asp residue should accept H^+ from the PSB and lead to multiple H^+ transfer reactions. Reflecting these reactions, MrHR-T74D exhibited a significantly different photocycle from that of wild-type MrHR, as shown in Fig. 2b. In particular, the characteristic M intermediate appeared at a short wavelength (390 nm). This significant blueshift of the spectrum is the result of the deprotonation of PSB, indicating that the embedded Asp residue actually acts as a H^+ acceptor from the PSB. M is the specific intermediate for H^+ pumps and was never observed for Cl^- pumps, including wild-type MrHR (Fig. 2a, 390 nm). For MrHR-T74D, M formation was completed within 20 μs (Fig. 2b, 390 nm), which is comparable to or faster than that of natural H^+ pumps. This H^+ transfer requires the inversion of the pKa values of the PSB and the acceptor Asp74 residue. In the dark state, the PSB has a larger pKa than that of the Asp residue. As a result, they are protonated and deprotonated. However, upon illumination, their pKa values are inverted so that H^+ can move from PSB to the Asp residue. These results suggested that MrHR-T74D conserves the structure and structural changes suitable for the primary H^+ transfer reaction. This view was further supported by the substantially low pKa of ~2.0 of the acceptor residue in the dark state (our unpublished result), which is comparable to the 2.6 pKa of BR [43]. This pKa value defines the lowest pH, where the Asp residue can act as a H^+ acceptor. Thus, MrHR-T74D can drive the H^+ transfer reaction even at very low pH, similar to BR.

In addition to the formation of M, the subsequent processes of MrHR-T74D are also notable. As shown in Fig. 2b, M decay leads to the formation of two intermediates corresponding to N (480 nm) and O (600 nm) in natural H^+ pumps. The M to N transition corresponds to the H^+ transfer from the donor to the SB, whereas the N to O transition corresponds to the H^+ uptake by the donor from the CP medium. For MrHR-T74D, both transitions occur at almost comparable rates to those of natural H^+ pumps. Thus, the third "D" residue in the TSD motif (Asp85) should act as an excellent H^+ donor in this mutant. As shown in Fig. 2c, its replacement by Asn (MrHR-T74D/D85N) greatly slowed M decay, indicating that

the Asp85 residue surely donates H^+ to the deprotonated SB. As shown in Fig. 2b, M, N and O sequentially appear without the formation of quasi-equilibria. This result probably reflects strict accessibility switching of the donor residue. During the M to N transition, the donor probably communicates only with the SB. After H^+ donation, strict accessibility switching seems to occur so that the donor in turn communicates only with the CP medium. This strict switching should be advantageous for one-way H^+ translocation. For BR, H^+ uptake by the donor becomes slower above pH~7.5, reflecting a pKa of 7~8 for H^+ uptake from the medium [44, 45]. As a result, M attains equilibrium with N, and they decay together, with a decay rate that is slower at higher pH [46]. However, for MrHR-T74D, the M decay rate was constant until pH 10, as shown in Fig. 2c. Above pH 10, M formation became negligible, probably due to the deprotonation of PSB. Thus, the donor of MrHR-T74D can capture H^+ from the medium at least until pH 10. As mentioned above, the third "D" residue (Asp85) has no potential role in the Cl^--pumping function of wild-type MrHR. However, upon introduction of the T74D mutation, the third "D" residue begins to act as an excellent H^+ donor residue.

As mentioned above, MrHR also conserves the PRG in BR, which is a pair of Glu194 and Glu204 in BR (Fig. 1a) and releases H^+ to the EC medium. This pair is conserved as Glu182 and Glu192 in MrHR (Fig. 1c). For BR, the primary H^+ transfer triggers the deprotonation of PRG via displacement of the Arg82 residue, located between the H^+ acceptor Asp85 and the PRG (Fig. 1a). This H^+ release occurs just after M formation and thus proceeds with H^+ uptake from the CP medium. Similar H^+ release prior to H^+ uptake was also observed for MrHR-T74D above pH 5.5 (our unpublished results), although the timing was different. For MrHR-T74D, H^+ release occurred at M decay or later. When either Glu182 or Glu192 was replaced by Gln, the fast H^+ release disappeared, indicating that this pair indeed acts as a PRG similar to that of BR. During the Cl^--pumping photocycle of wild-type MrHR, neither Glu residue changed its protonation state [33]. Thus, this pair begins to act as a PRG when the T74D mutation is introduced. These results indicated that MrHR conserves a mechanism in BR that connects primary H^+ transfer and subsequent H^+ release from the PRG.

Optimizations Required for MrHR to Become a Mature Cl^- Pump

As mentioned above, MrHR conserves the residues characteristic of the BR-type H^+ pump. The representatives are the H^+ donor residue and the PRG. These residues have no potential role in the Cl^--pumping function but begin to work upon embedding the H^+ acceptor residue for the H^+ pump. These results seem to reflect poor optimization of the residues and structure in MrHR toward efficient Cl^- pumps such as NpHR. Thus, differences between MrHR and NpHR might be related to optimization to become efficient Cl^- pumps. The distinct difference is the decay rate of the last intermediate. The decay of MrHR′ is notably slow compared to NpHR′. Some optimization is necessary to accelerate the MrHR′ decay and to subsequently elevate the Cl^--pumping efficiency.

The other characteristic difference was suggested to be the protonation state of the Asp200 residue in the vicinity of PSB (Fig. 1g) [33]. This Asp residue is superconserved in most microbial rhodopsins and is considered to be deprotonated in the dark state. This is also true for NpHR [33]. When the corresponding Asp252 in NpHR was replaced by Asn, significant changes appeared in the dark state (Fig. 4a, b): The absorption spectra in both the Cl^--free form and Cl^--binding form exhibited distinct blueshifts (52 nm in the Cl^--free form and 11 nm in the Cl^--binding form). Moreover, the direction of the Cl^--induced spectral shift was also modified (Fig. 4a, b): For wild-type NpHR, Cl^- binding caused a spectral blueshift (Fig. 4a), whereas the opposite redshift was observed for NpHR-D252N (Fig. 4b). Thus, the Asp252 residue is indeed deprotonated in wild-type NpHR. In contrast, for MrHR, the corresponding D200N mutation did not affect the absorption spectra in either Cl^--free or Cl^--binding forms (Fig. 4c, d). Moreover, both the wild-type and the D200N mutant exhibited a spectral redshift upon Cl^- binding, similar to NpHR-D252N (Fig. 4b). Thus, Asp200 in MrHR is probably protonated in the dark state.

As mentioned above, Cl^- and key residues around PSB are located at similar positions in MrHR and NpHR (Fig. 1f, g). This is also true for Asp200 of MrHR and Asp252 of NpHR. Thus, the difference in their protonation states appears to be inconsistent with the structural similarity. Based on analogy with BR [25], the deprotonated Asp252 of NpHR seems to be stabilized by the positive charge of Arg123 and the hydrogen bonding interactions with Tyr82, Tyr225 and water molecules (Supplementary Figure S1a, c). MrHR also conserves the corresponding residues, Arg71, Tyr50, and Tyr173, and partly conserves water molecules (Supplementary Figure S1b, d), but the significance of Arg71 is probably different. For NpHR, the replacement of Arg123 by neutral residues greatly distorts the photocycle and completely removes the Cl^--pumping activity [47]. However, for MrHR, the corresponding mutation did not induce a significant effect [33]. MrHR-R71Q still showed almost the same photocycle as wild-type MrHR and maintained distinct Cl^--pumping activity, indicating that the positive charge of Arg71 has no significant influence on the surrounding environment. Thus, in MrHR, Arg71 might not promote the deprotonation of the Asp200 residue, although these residues take almost the same positions as their counterparts in NpHR (Fig. 1f, g).

For MrHR, the D200N mutation did not distort the electrostatic environment, as mentioned above. However, this mutation also removed the Cl^--pumping activity, similar to NpHR [33, 48]. Thus, photolyzed MrHR probably needs to deprotonate the Asp200 residue to drive Cl^- transport. This Asp residue is located on the EC side of the PSB (Fig. 1g),

which connects to the EC medium via a hydrophilic channel. Thus, the H^+ from Asp200 seems to be ejected to the EC medium. Indeed, for wild-type MrHR, transient H^+ release was observed during L decay [33]. Conversely, for MrHR-D200N, the photocycle lacked both H^+ release and the formation of intermediates after L [33]. Thus, for wild-type MrHR, the Asp200 residue deprotonates during L decay. The resultant negative charge is necessary to eject Cl^- toward the CP side and to prompt the photocycle over the L intermediate. This mechanism is probably common to NpHR because its D252N mutant also lacked Cl^--pumping activity. For NpHR, the negative charge at the 252nd position already exists in the dark state and undergoes photocycle while maintaining the deprotonated state. Conversely, for MrHR, Asp200 might need to protonate for strong Cl^- binding in the dark state. Even in this case, MrHR can transport Cl^- by deprotonating the Asp200 residue. However, the resultant dipole moment upon H^+ release might be a problem. This dipole moment is likely to disturb Cl^- movement toward the CP side and/or the uptake of new Cl^- from the EC medium. In other words, for NpHR, the PSB region is optimized so that Cl^- can strongly bind even in the presence of a negative charge of Asp252. This optimization might be related to the stronger influence of the positive charge of Arg123.

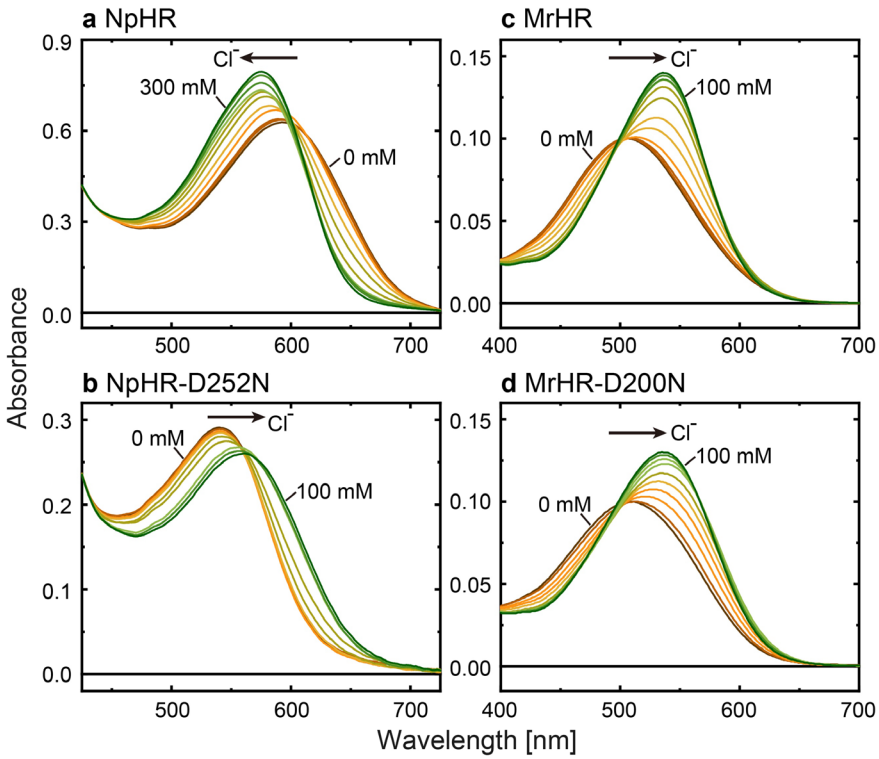

Figure 4 The difference in the protonation state of Asp252 in NpHR and Asp200 in MrHR. Cl^--induced absorption spectral shifts are plotted. For NpHR (left panels), the wild-type protein exhibited a spectral blueshift (a), whereas the D252N mutant exhibited an "opposite" redshift (b). Conversely, for MrHR (right panels), both the wild-type protein (c) and the D200N mutant (d) exhibited a redshift similar to the D252N NpHR (b). The Cl^- concentrations were changed from 0 mM to 300 mM for wild-type NpHR (a) and from 0 mM to 100 mM for other samples. Adapted from [33], Copyright (2018), with permission from Elsevier.

Physiological Roles of MrHR

MrHR seems to be an immature Cl^- pump that just differentiated from the BR-type H^+ pump. Why was MrHR poorly optimized compared to other matured Cl^- pumps? Poor maturation should be related to the physiological role of this protein. In addition to MrHR, the physiological role of other Cl^- pumps has not been fully clarified. One possibility is the contribution to ATP production. Inward Cl^- transport strengthens the electrochemical gradient of H^+ and thus can facilitate ATP production by H^+-driven ATP synthase. Stronger Cl^- pumps make a greater contribution to ATP production. Thus, Cl^- pumps should be optimized to exert strong activity. This does not seem to be true for MrHR. This Cl^- pump probably has a different role than ATP production. Indeed, MrHR is encoded in cyanobacteria, which contain a photosynthetic apparatus and can efficiently utilize light energy without the help of MrHR. The other possibility might be a contribution

to survival under drought stress. The host cyanobacterium inhabits the soil and is often exposed to drought stress. Under this condition, the increase in CP salt concentration should contribute to maintaining the water content. Due to the interior negative membrane potential, cations can easily move inside the cell. However, for the uptake of the counteranions, an active transport mechanism such as MrHR seems to be necessary. This role might not require strong Cl^- transport, so the Cl^--pumping mechanism of MrHR might be poorly optimized.

Concluding Remarks

Previous FT-IR analyses pointed out that H^+-pump rhodopsins commonly require a strongly hydrogen-bonded water molecule in the PSB region [42]. This view was nicely confirmed by the structure of MrHR-T74D (Fig. 1h), which contains a water molecule that connects the PSB and two Asp residues at close distances (< 3.0 Å) [35]. This water was originally present in wild-type MrHR at almost the same position as in the mutant (Fig. 1g). Similar water molecule also exists in NpHR (Fig. 1f), but it is far from the surrounding components. Thus, the presence of characteristic water molecules was concluded to be related to the easy conversion of MrHR into a H^+ pump [35].

MrHR seems to be close to an ancestor of NpHR. Their structures around PSB might reflect this molecular evolution. As shown in Fig. 1f and g, MrHR contains a simple hydrogen bonding network, whereas NpHR forms an extensive network with additional water molecules. A similar difference also exists between MrHR-T74D and BR (Fig. 1e and h). The former contains a simple hydrogen bonding network, which is in clear contrast to the extensive network in BR. This difference might be related to the lower H^+ pumping ability of MrHR-T74D. Previous study showed that MrHR-T74D is a weak H^+ pump because the last intermediate in the photocycle has substantially slow decay, similar to MrHR´ in the wild-type photocycle [8]. Moreover, the photocycle of MrHR-T74D has a branch that does not involve N and O intermediates and thus probably lacks H^+ pumping activity [8]. Therefore, a comparative study not only between MrHR and NpHR, but also between MrHR-T74D and BR would be interesting. They might contribute to a deeper understanding of respective strategies for creating excellent Cl^- and H^+ pumps. The differences in the hydrogen bonding networks in the PSB regions would be of initial interests in those studies.

Conflict of Interest

The author declares that there are no conflicts of interest.

Author Contributions

T. K. wrote the manuscript.

Acknowledgements

This work was supported by the Japan Society for the Promotion of Science KAKENHI (17K07326, 26440042) and the Akiyama Life Science Foundation.

References

[1] Unno, M., Hirose, Y., Mishima, M., Kikukawa, T., Fujisawa, T., Iwata, T., et al. Spectroscopic approach for exploring structure and function of photoreceptor proteins. Biophys. Physicobiol. 18, 127-130 (2021). https://doi.org/10.2142/biophysico.bppb-v18.014

[2] Ernst, O.P., Lodowski, D.T., Elstner, M., Hegemann, P., Brown, L.S., Kandori, H. Microbial and animal rhodopsins: structures, functions, and molecular mechanisms. Chem. Rev. 114, 126-163 (2014). https://doi.org/10.1021/cr4003769

[3] Govorunova, E.G., Sineshchekov, O.A., Li, H., Spudich, J.L. Microbial rhodopsins: Diversity, mechanisms, and optogenetic applications. Annu. Rev. Biochem. 86, 845-872 (2017). https://doi.org/10.1146/annurev-biochem-101910-144233

[4] Kandori, H. Biophysics of rhodopsins and optogenetics. Biophys. Rev. 12, 355-361 (2020). https://doi.org/10.1007/s12551-020-00645-0

[5] Spudich, J.L., Yang, C.S., Jung, K.H., Spudich, E.N. Retinylidene proteins: Structures and functions from archaea to humans. Annu. Rev. Cell Dev. Biol. 16, 365-392 (2000). https://doi.org/10.1146/annurev.cellbio.16.1.365

[6] Spudich, J.L., Jung, K.H. Microbial rhodopsin: Phylogenetic and functional diversity. in Hand book of photosensory receptors. (Briggs, W.R., Spudich, J.L. eds.), pp. 1-23 (Wiley-VCH Verlag, Weinheim, 2005).

[7] Rozenberg, A., Inoue, K., Kandori, H., Béjà, O. Microbial rhodopsins: The last two decades. Annu. Rev. Microbiol. 75, 427-447 (2021). https://doi.org/10.1146/annurev-micro-031721-020452
[8] Hasemi, T., Kikukawa, T., Kamo, N., Demura, M. Characterization of a cyanobacterial chloride-pumping rhodopsin and its conversion into a proton pump. J. Biol. Chem. 291, 355-362 (2016). https://doi.org/10.1074/jbc.M115.688614
[9] Oesterhelt, D., Stoeckenius, W. Rhodopsin-like protein from the purple membrane of *Halobacterium halobium*. Nature 233, 149-152 (1971). https://doi.org/10.1038/newbio233149a0
[10] Oesterhelt, D., Stoeckenius, W. Functions of a new photoreceptor membrane. Proc. Natl. Acad. Sci. U.S.A. 70, 2853-2857 (1973). https://doi.org/10.1073/pnas.70.10.2853
[11] Matsuno-Yagi, A., Mukohata, Y. Two possible roles of bacteriorhodopsin; a comparative study of strains of *Halobacterium halobium* differing in pigmentation. Biochem. Biophys. Res. Commun. 78, 237-243 (1977). https://doi.org/10.1016/0006-291X(77)91245-1
[12] Schobert, B., Lanyi, J.K. Halorhodopsin is a light-driven chloride pump. J. Biol. Chem. 257, 10306-10313 (1982). https://doi.org/10.1016/S0021-9258(18)34020-1
[13] Bogomolni, R.A., Spudich, J.L. Identification of a third rhodopsin-like pigment in phototactic *Halobacterium halobium*. Proc. Natl. Acad. Sci. U.S.A. 79, 6250-6254 (1982). https://doi.org/10.1073/pnas.79.20.6250
[14] Takahashi, T., Tomioka, H., Kamo, N., Kobatake, Y. A photosystem other than PS370 also mediates the negative phototaxis of *Halobacterium halobium*. FEMS Microbiol. Lett. 28, 161-164 (1985). https://doi.org/10.1111/j.1574-6968.1985.tb00784.x
[15] Bieszke, J.A., Braun, E.L., Bean, L.E., Kang, S., Natvig, D.O., Borkovich, K.A. The nop-1 gene of *Neurospora crassa* encodes a seven transmembrane helix retinal-binding protein homologous to archaeal rhodopsins. Proc. Natl. Acad. Sci. U.S.A. 96, 8034-8039 (1999). https://doi.org/10.1073/pnas.96.14.8034
[16] Yoshizawa, S., Kumagai, Y., Kim, H., Ogura, Y., Hayashi, T., Iwasaki, W., et al. Functional characterization of flavobacteria rhodopsins reveals a unique class of light-driven chloride pump in bacteria. Proc. Natl. Acad. Sci. U.S.A. 111, 6732-6737 (2014). https://doi.org/10.1073/pnas.1403051111
[17] Hosaka, T., Yoshizawa, S., Nakajima, Y., Ohsawa, N., Hato, M., DeLong, E.F., et al. Structural mechanism for light-driven transport by a new type of chloride ion pump, *Nonlabens marinus* rhodopsin-3. J. Biol. Chem. 291, 17488-17495 (2016). https://doi.org/10.1074/jbc.M116.728220
[18] Kim, K., Kwon, S.K., Jun, S.H., Cha, J.S., Kim, H., Lee, W., et al. Crystal structure and functional characterization of a light-driven chloride pump having an NTQ motif. Nat. Commun. 7, 12677 (2016). https://doi.org/10.1038/ncomms12677
[19] Kato, H.E., Inoue, K., Abe-Yoshizumi, R., Kato, Y., Ono, H., Konno, M., et al. Structural basis for Na^+ transport mechanism by a light-driven Na^+ pump. Nature 521, 48-53 (2015). https://doi.org/10.1038/nature14322
[20] Gushchin, I., Shevchenko, V., Polovinkin, V., Kovalev, K., Alekseev, A., Round, E., et al. Crystal structure of a light-driven sodium pump. Nat. Struct. Mol. Biol. 22, 390-395 (2015). https://doi.org/10.1038/nsmb.3002
[21] Duschl, A., Lanyi, J.K., Zimányi, L. Properties and photochemistry of a halorhodopsin from the haloalkalophile, *Natronobacterium pharaonis*. J. Biol. Chem. 265, 1261-1267 (1990). https://doi.org/10.1016/S0021-9258(19)40007-0
[22] Seki, A., Miyauchi, S., Hayashi, S., Kikukawa, T., Kubo, M., Demura, M., et al. Heterologous expression of *pharaonis* halorhodopsin in *Xenopus laevis* oocytes and electrophysiological characterization of its light-driven Cl^- pump activity. Biophys. J. 92, 2559-2569 (2007). https://doi.org/10.1529/biophysj.106.093153
[23] Inoue, K., Koua, F.H.M., Kato, Y., Abe-Yoshizumi, R., Kandori, H. Spectroscopic study of a light-driven chloride ion pump from marine bacteria. J. Phys. Chem. B 118, 11190-11199 (2014). https://doi.org/10.1021/jp507219q
[24] Niho, A., Yoshizawa, S., Tsukamoto, T., Kurihara, M., Tahara, S., Nakajima, Y., et al. Demonstration of a light-driven SO_4^{2-} transporter and its spectroscopic characteristics. J. Am. Chem. Soc. 139, 4376-4389 (2017). https://doi.org/10.1021/jacs.6b12139
[25] Balashov, S.P. Protonation reactions and their coupling in bacteriorhodopsin. Biochim. Biophys. Acta 1460, 75-94 (2000). https://doi.org/10.1016/s0005-2728(00)00131-6
[26] Lanyi, J.K. Bacteriorhodopsin. Annu. Rev. Physiol. 66, 665-688 (2004). https://doi.org/10.1146/annurev.physiol.66.032102.150049
[27] Sasaki, S., Tamogami, J., Nishiya, K., Demura, M., Kikukawa, T. Replaceability of Schiff base proton donors in light-driven proton pump rhodopsins. J. Biol. Chem. 101013 (2021). https://doi.org/10.1016/j.jbc.2021.101013
[28] Kikukawa, T. Functional mechanism of Cl^--pump rhodopsin and its conversion into H^+ pump. in Optogenetics: Light-Sensing Proteins and Their Applications in Neuroscience and Beyond. (Yawo, H., Kandori, H., Koizumi, A., Kageyama, R. eds.), pp. 55-71 (Springer Singapore, Singapore, 2021).
[29] Sato, M., Kikukawa, T., Araiso, T., Okita, H., Shimono, K., Kamo, N., et al. Roles of Ser130 and Thr126 in chloride binding and photocycle of *pharaonis* halorhodopsin. J. Biochem. 134, 151-158 (2003).

https://doi.org/10.1093/jb/mvg123
[30] Sato, M., Kikukawa, T., Araiso, T., Okita, H., Shimono, K., Kamo, N., et al. Ser-130 of *Natronobacterium pharaonis* halorhodopsin is important for the chloride binding. Biophys. Chem. 104, 209-216 (2003). https://doi.org/10.1016/s0301-4622(02)00368-x
[31] Sato, M., Kubo, M., Aizawa, T., Kamo, N., Kikukawa, T., Nitta, K., et al. Role of putative anion-binding sites in cytoplasmic and extracellular channels of *Natronomonas pharaonis* halorhodopsin. Biochemistry 44, 4775-4784 (2005). https://doi.org/10.1021/bi047500f
[32] Kouyama, T., Kawaguchi, H., Nakanishi, T., Kubo, H., Murakami, M. Crystal structures of the L_1, L_2, N, and O states of *pharaonis* halorhodopsin. Biophys. J. 108, 2680-2690 (2015). https://doi.org/10.1016/j.bpj.2015.04.027
[33] Hasemi, T., Kikukawa, T., Watanabe, Y., Aizawa, T., Miyauchi, S., Kamo, N., et al. Photochemical study of a cyanobacterial chloride-ion pumping rhodopsin. Biochim. Biophys. Acta Bioenerg. 1860, 136-146 (2019). https://doi.org/10.1016/j.bbabio.2018.12.001
[34] Yun, J.H., Park, J.H., Jin, Z., Ohki, M., Wang, Y., Lupala, C.S., et al. Structure-based functional modification study of a cyanobacterial chloride pump for transporting multiple anions. J. Mol. Biol. 432, 5273-5286 (2020). https://doi.org/10.1016/j.jmb.2020.07.016
[35] Besaw, J.E., Ou, W.L., Morizumi, T., Eger, B.T., Sanchez Vasquez, J.D., Chu, J.H.Y., et al. The crystal structures of a chloride-pumping microbial rhodopsin and its proton-pumping mutant illuminate proton transfer determinants. J. Biol. Chem. 295, 14793-14804 (2020). https://doi.org/10.1074/jbc.RA120.014118
[36] Kikukawa, T., Kusakabe, C., Kokubo, A., Tsukamoto, T., Kamiya, M., Aizawa, T., et al. Probing the Cl^--pumping photocycle of *pharaonis* halorhodopsin: Examinations with bacterioruberin, an intrinsic dye, and membrane potential-induced modulation of the photocycle. Biochim. Biophys. Acta 1847, 748-758 (2015). https://doi.org/10.1016/j.bbabio.2015.05.002
[37] Hasegawa, C., Kikukawa, T., Miyauchi, S., Seki, A., Sudo, Y., Kubo, M., et al. Interaction of the halobacterial transducer to a halorhodopsin mutant engineered so as to bind the transducer: Cl^- circulation within the extracellular channel. Photochem. Photobiol. 83, 293-302 (2007). https://doi.org/10.1562/2006-06-09-RA-916
[38] Lazarova, T., Sanz, C., Querol, E., Padrós, E. Fourier transform infrared evidence for early deprotonation of Asp^{85} at alkaline pH in the photocycle of bacteriorhodopsin mutants containing E194Q. Biophys. J. 78, 2022-2030 (2000). https://doi.org/10.1016/S0006-3495(00)76749-X
[39] Sasaki, J., Brown, L.S., Chon, Y.S., Kandori, H., Maeda, A., Needleman, R., et al. Conversion of bacteriorhodopsin into a chloride ion pump. Science 269, 73-75 (1995). https://doi.org/10.1126/science.7604281
[40] Havelka, W.A., Henderson, R., Oesterhelt, D. Three-dimensional structure of halorhodopsin at 7 Å resolution. J. Mol. Biol. 247, 726-738 (1995). https://doi.org/10.1016/S0022-2836(05)80151-2
[41] Váró, G., Brown, L.S., Needleman, R., Lanyi, J.K. Proton transport by halorhodopsin. Biochemistry 35, 6604-6611 (1996). https://doi.org/10.1021/bi9601159
[42] Muroda, K., Nakashima, K., Shibata, M., Demura, M., Kandori, H. Protein-bound water as the determinant of asymmetric functional conversion between light-driven proton and chloride pumps. Biochemistry 51, 4677-4684 (2012). https://doi.org/10.1021/bi300485r
[43] Balashov, S.P., Govindjee, R., Kono, M., Imasheva, E., Lukashev, E., Ebrey, T.G., et al. Effect of the arginine-82 to alanine mutation in bacteriorhodopsin on dark adaptation, proton release, and the photochemical cycle. Biochemistry 32, 10331-10343 (1993). https://doi.org/10.1021/bi00090a008
[44] Balashov, S.P., Lu, M., Imasheva, E.S., Govindjee, R., Ebrey, T.G., Othersen, B., 3rd, et al. The proton release group of bacteriorhodopsin controls the rate of the final step of its photocycle at low pH. Biochemistry 38, 2026-2039 (1999). https://doi.org/10.1021/bi981926a
[45] Tamogami, J., Kikukawa, T., Miyauchi, S., Muneyuki, E., Kamo, N. A tin oxide transparent electrode provides the means for rapid time-resolved pH measurements: application to photoinduced proton transfer of bacteriorhodopsin and proteorhodopsin. Photochem. Photobiol. 85, 578-589 (2009). https://doi.org/10.1111/j.1751-1097.2008.00520.x
[46] Otto, H., Marti, T., Holz, M., Mogi, T., Lindau, M., Khorana, H.G., et al. Aspartic acid-96 is the internal proton donor in the reprotonation of the Schiff base of bacteriorhodopsin. Proc. Natl. Acad. Sci. U.S.A. 86, 9228-9232 (1989). https://doi.org/10.1073/pnas.86.23.9228
[47] Kubo, M., Kikukawa, T., Miyauchi, S., Seki, A., Kamiya, M., Aizawa, T., et al. Role of Arg123 in light-driven anion pump mechanisms of *pharaonis* halorhodopsin. Photochem. Photobiol. 85, 547-555 (2009). https://doi.org/10.1111/j.1751-1097.2009.00538.x
[48] Chen, X.R., Huang, Y.C., Yi, H.P., Yang, C.S. A Unique light-driven proton transportation signal in halorhodopsin from *Natronomonas pharaonis*. Biophys. J. 111, 2600-2607 (2016). https://doi.org/10.1016/j.bpj.2016.11.003